Use of a magnetic field to increase the spatial resolution of positron emission tomography

Bruce E. Hammer
Department of Radiology, University of Minnesota, 420 Delaware Street, Minneapolis, Minnesota 55455

Nelson L. Christensen and Brian G. Heil
Department of Physics, University of Minnesota, 116 Church Street SE, Minneapolis, Minnesota 55455

(Received 19 January 1994; accepted for publication 8 August 1994)

Detector geometry, spatial sampling, and more fundamentally, positron range and noncollinearity of annihilation photon emission define Positron Emission Tomography (PET) spatial resolution. In this paper, a strong magnetic field is used to constrain positron travel transverse to the field. Measurement of the spread function from a 500 μm diameter ^{68}Ga impregnated resin bead shows a squeezing of the full width at half maximum (FWHM) by a factor of 1.0, 1.22, 1.42, and 2.05, at 0, 4.0, 5.0, and 9.4 Tesla, respectively. The full width at tenth maximum (FWTM) decreases by a factor of 1.0, 1.73, 2.09, and 3.20, at 0, 4.0, 5.0, and 9.0 Tesla, respectively. Acquiring a PET image in a magnetic field should significantly reduce resolution loss due to positron range.

Key words: positron, range, magnetic field, photodiode

I. INTRODUCTION

Functional imaging of the brain by Positron Emission Tomography (PET) and Magnetic Resonance Imaging (MRI) techniques yield insight into the correlation of brain activity with neuronal activity, blood flow, and oxygenation.[1-3] In light of recent functional MRI and PET applications it would be of great scientific interest to obtain PET and MRI images of a subject at the same time and in the same scanner.[4] At first glance combining these two modalities into one unit appears to be mutually exclusive because PET scanners typically use photomultiplier tubes that do not function well in magnetic fields and MR scanners cannot have ferromagnetic materials within the magnet's bore. A number of investigators use photodiodes and avalanche photodiodes for PET applications.[5,6] These devices are physically small, electrically stable, and magnetic field tolerant.[7,8] As a first step toward our long-term objective of combining PET and MRI technologies into one unit we examine the feasibility of detecting positron annihilation in a strong magnetic field using commercially available photodiode detectors. We also examine the effect of magnetic field on the positron range.

II. MATERIALS AND METHODS

A 500 μm diameter microsphere resin bead impregnated with 100 μCi of ^{68}Ga or ^{22}Na (Isotope Products Laboratories, Berkeley, CA) is in the center of a 2.5×2.5 cm cylinder of tissue equivalent wax (Radiation Products Design, Inc., Albertsville, MN). A pair of opposing 28×28×28 mm CsI scintillators that mounts to 18×18 mm photodiode (EV Products, Saxon, PA) detectors operating at +42 V bias detects the annihilation photons. A cylindrical lead collimator (50×50 mm) with a 1 mm wide×25 mm high slit resides between the sample and detectors. Distance from source to end of collimator is 82 mm. The radioactive sample mounts to a nonmagnetic movable platform (Velmex, East Bloomfield, NY) and resides in the center of either a 4.0 T/1.25 m (Siemens Medical, Erlangen, Germany), 5.0 T/0.4 m (Magnex Scientific LTD, Abingdon, England) or 9.4 T/0.3 m (Magnex Scientific LTD., Abingdon, England) magnet. The magnetic field uniformity over the sample and radiation detectors varies less than 0.001%. Translation of the source past the detectors and the recording of coincidence count rate as a function of position yields the spread function.[9,10] Equipment used for coincidence measurements (Tennelec/Nucleus Inc., Oak Ridge, TN): Two TC-241 amplifiers; two TC-450 single channel analyzers; one TC-404A multipurpose coincidence unit; one TC-532 counter; one TB-3 chassis.

One hour prior to each experiment the photodiode detectors and electronics equilibrate to the ambient temperature of the surrounds because photodiode gain is temperature dependent. The temperature variation for each experiment varies less than 1 deg from start to finish. No measurable change in detector gain is apparent for changes in temperature of less than 5 °C. To establish the position of the 0.511 MeV photopeak a gamma ray spectrum (Tennelec PCAII multichannel analyzer) is acquired from each detector with the source in the center of the collimator slit. The TC-450 discriminators are set to the 0.511 MeV photopeak with a 0.065 MeV window [full width at half maximum (FWHM)]. Photodiode detector energy resolution (=centroid/FWHM) and gain was measured at 0, 4.0, 5.0, and 9.4 T. Based on three measurements at each field, for each photodiode detector, the energy resolution is 12.4±1.0% and 12.5±1.4% at a 95% confidence level, respectively. Measurement of detector gain as a function of field strength utilized a 0.5 uCi ^{22}Na check source placed on top of each detector. The ^{22}Na source contains a 1 cm diameter active region imbedded in a plastic disk. Total counts under the photopeak varied less than 5% for all measured fields. Photodiode gain and resolution are therefore field independent up until at least 9.4 T.

To measure the maximum squeezing of positron range the long axis of each photodiode detector is aligned parallel to the magnetic field, which orients along the z axis in Fig. 1. Translating the sample perpendicular to field lines (i.e., along the x axis) measures the spread function of positrons having momentum components perpendicular to the magnetic field. This orientation applies to measurements at 4.0, 5.0, and 9.4

 0094-2405/94/21(12)/1917/4/$1.20

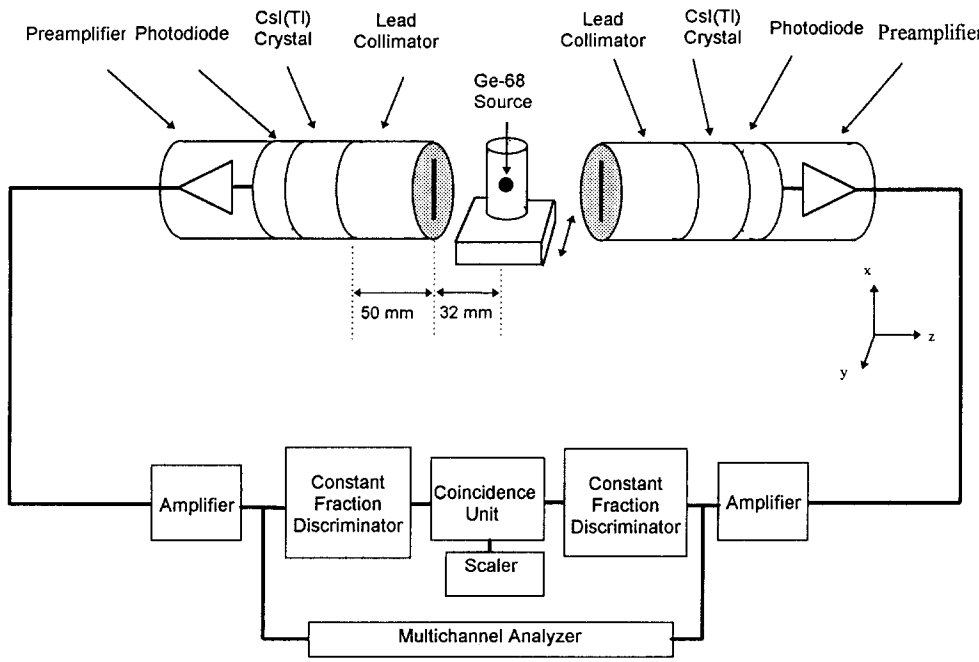

FIG. 1. Schematic diagram of the equipment used for measuring positron range. The preamplifier, photodiode, CsI(Tl) crystal, lead collimator and ^{68}Ga source are in the center of an MRI magnet for measurements in a magnetic field. The magnetic field is along the z axis for most measurements.

T. Rotating the apparatus by 90° places the axis connecting the photodiode detectors perpendicular to the field. Translating the sample parallel to the field allows measurement of positrons with momentum components parallel to the field. In this orientation the magnetic field does not affect positron range. Only the 4.0 T magnet has a bore large enough to accommodate a measurement parallel to the field. Experimental resolution was determined by placing ^{18}F, which is a low energy positron emitter, in a 220 μm i.d. borosilicate tube with a wall thickness of 1 mm (Polymicro Technologies, Phoenix, AZ). The wall thickness was great enough to stop the most energetic positrons. Measurement of line spread function was identical to the method used for ^{68}Ga and ^{22}Na measurements.

III. RESULTS AND DISCUSSION

The coincident detection of the two antiparallel 0.511 MeV photons resulting from positron–electron annihilation forms the basis of PET imaging. Angular deviation of annihilation photons and the radial distance a positron travels before annihilation determines the intrinsic resolution of a PET image.[11–14] Use of small diameter detector rings minimizes the effect of noncollinearity of annihilation photons whereas a strong magnetic field limits the range of positrons that travel transverse to the field.

Positron range is dependent on positron energy and composition of the medium through which it travels. In tissue the only means to limit positron range is to utilize a low energy positron emitter, e.g., ^{22}Na (E_{max}=0.51 MeV) or ^{18}F (E_{max}=0.635 MeV), which may not be suitable for many experimental scenarios.[15] Higher energy positron emitters in wide scale use include ^{11}C (E_{max}=0.97 MeV), ^{13}N (E_{max}=1.20 MeV), ^{15}O (E_{max}=1.74 MeV), ^{68}Ga (E_{max}=1.90 MeV), and ^{82}Rb (E_{max}=3.15 MeV). Positrons from these isotopes travel millimeters from the source before annihilation. This leads to significant blurring of the PET image.

Measuring the variation of point spread or line spread function as a function of positron energy and density of medium yields an estimate of positron range in matter.[9,10] Translating a positron source past a pair of opposed lead-collimated scintillation detectors and recording coincident events, as a function of position, in a 0.511±0.032 MeV energy window results in a curve that approximates a Gaussian function. One method of experimentally measuring positron range is based on measuring the FWHM or FWTM (full width tenth maximum) of a spread function.[16]

The apparatus shown in Fig. 1 measures the spread function at field strengths of 0, 4.0, 5.0, and 9.4 T. The radial distribution of annihilation events from an isotopic emission of positrons is a convolution of the positron energy spectrum with the distribution of radial distances a specific energy positron travels before annihilation. Imposition of a strong magnetic field decreases the radial distance of positron travel transverse to the field[4,17] whereas positron range longitudinal to the field is unaffected;[4] Fig. 2 demonstrates this effect. The FWHM of positrons with momentum components perpendicular and parallel to the field is 1.88±0.05 mm and 2.32±0.05 mm, respectively. Note the spread function of positrons traveling parallel to the field is identical to zero field measurements (Table I).

Figure 3 shows the change in the spread function for ^{68}Ga at different magnetic field strengths. At increasing magnetic fields the FWHM decreases indicating that positron range transverse to the magnetic field has decreased (Table I). For the ^{68}Ga source the positron range dominates the FWHM and FWTM of the spread function; twice the cyclotron radius[18]

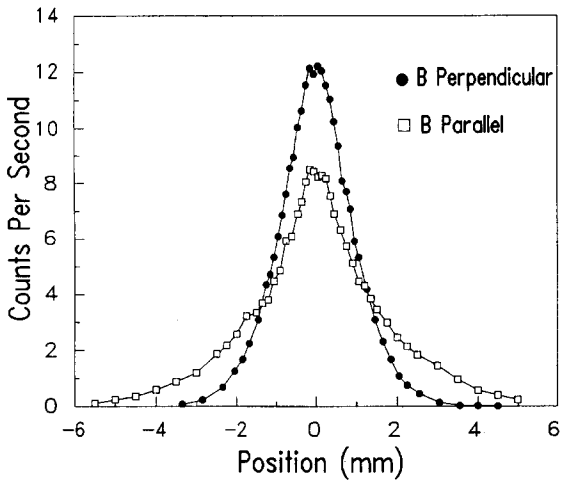

FIG. 2. Demonstration of asymmetry of annihilation zone around a 500 μm bead coated with 100 μCi of ^{68}Ga in a 4.0 T magnetic field. Translating the sample perpendicular to field lines (i.e., ● B Perpendicular in plot) measures the spread function of positrons with momentum components perpendicular to the magnetic field. Rotating the apparatus by 90° places the axis connecting the photodiode detectors perpendicular to the field. Translating the sample parallel to the field allows measurement of positrons with momentum components parallel to the field (i.e., □ B Parallel in plot).

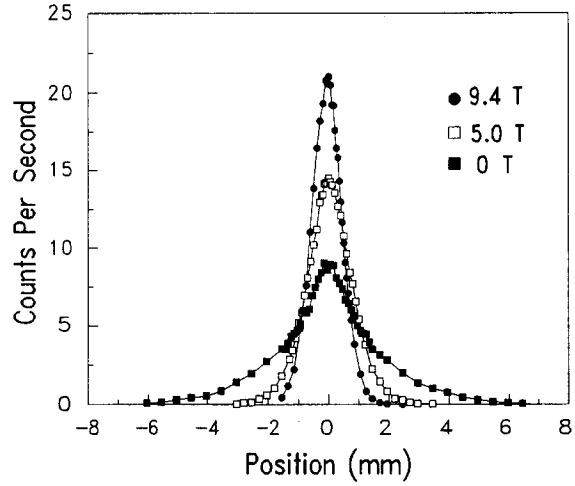

FIG. 3. Measurement of the spread function from a 500 μm diameter ^{68}Ga bead at 0, 5.0, and 9.4 T yields a FWHM of 2.3, 1.6, and 1.1 mm and FWTM of 7.2, 3.4, and 2.2 mm, respectively. Moving the sample perpendicular to the field, past the collimated detectors whose long axes are parallel to the field, yields the spread function. A narrowing of the measured spread function occurs because the magnetic field limits the distance a positron travels perpendicular to the magnetic field.

(R) for the average and maximum positron energy, respectively, plus the bead diameter gives an approximate value for the FWHM and FWTM, respectively, i.e., FWHM=2R +bead diameter where $R=P(\text{MeV/c})/29980*B(T)$. A positron with momentum P(eV/c), moving transverse to the magnetic field (T), moves in a circular orbit with a radius given by the previous formula. In condensed matter the orbit radius decreases because of energy loss due to ionizations and excitations. Detector geometry and the slight noncolinearity of the two coincident gamma photons are the dominant contributions to the spread function's FWHM and FWTM for relatively low energy ^{22}Na positrons.

The FWHM is most sensitive to the median positron energy range. The FWTM also shows a significant decrease at higher field strengths and is most sensitive to higher energy positron range. Measurement of the spread function from a 500 μm diameter ^{68}Ga bead at 0, 4.0, 5.0, and 9.4 T yields a decrease in FWHM by a factor of 1.0, 1.22, 1.42, and 2.05, and FWTM by a factor of 1.0, 1.73, 2.09, and 3.0, respectively. Figure 3 also shows that an increase in count rate is concomitant with a decrease in FWHM. This occurs because the density of positron annihilation increases with increasing magnetic field. The area under each curve is conserved to within experimental error.

TABLE I. FWHM and FWTM of positron annihilation spread function for ^{68}Ga and ^{22}Na coated 500 μm glass bead.

Isotope	Field (Tesla)	FWHM (mm)	FWTM (mm)
^{68}Ga[a]	0	2.30±0.10	7.10±0.10
^{68}Ga[b]	4.0	1.88±0.05	4.10±0.05
^{68}Ga[a]	5.0	1.62±0.05	3.40±0.05
^{68}Ga[c]	9.4	1.12±0.03	2.22±0.03
^{22}Na[b]	0	0.96±0.02	2.25±0.02
^{22}Na[b]	5.0	0.96±0.02	2.12±0.02
^{22}Na[b]	9.4	0.86±0.02	1.87±0.02

[a]Average of four scans.
[b]One scan.
[c]Average of three scans. Error for (a) and (c) based on composite error from individual scans. Error for (b) determined by propagating errors associated with individual points on the spread function.

The effect of magnetic field on the range of ^{22}Na positrons is scarcely measurable. ^{22}Na (E_{max}=0.545 MeV) has a very low range of positron energies[15] and consequently does not experience a strong Lorentz force in a magnetic field (Table I). The range of ^{22}Na positrons in the tissue-equivalent medium is comparable to the resolution inherent to the present experimental conditions.[19] The line spread function for ^{18}F (E_{max}=0.635 MeV) in a 220 μm i.d. Borosilicate tube had a FWHM of 0.79±0.02 mm and a FWTM of 1.49±0.02 mm. The maximum range of an ^{18}F positron is about 1.0 mm in borosilicate glass and the average range is approximately 0.3 mm.

IV. CONCLUSIONS

Acquiring a PET image in a strong magnetic field reduces the effect of positron range on image blurring. Use of small scintillation crystals, low noise detectors and smaller diameter rings can also enhance PET resolution. A small diameter PET ring for use in strong magnetic fields should allow for the imaging of small animals at submillimeter resolution that is not feasible with present-day scanners.

ACKNOWLEDGMENTS

The authors gratefully acknowledge the loan of nuclear instrumentation from Intermagnetics General Corporation, Latham, New York. We thank Dr. K. Ugurbil, Dr. M. Garwood, and Dr. H. Merkle for access to the 4.0 and 9.4 T magnets at the Center for Magnetic Resonance Research,

University of Minnesota, Minneapolis, MN. We also thank Dr. S. Strother, Dr. C. Arnet, and Dr. M. Sajjad from the PET imaging Section at the VA Medical Center, Minneapolis, MN, for supplying F-18 radioisotope. Supported by U. S. Public Service Grant (1 R03 RR07042-01) and University of Minnesota Grant-in-Aid Program.

[1]J. W. Belliveau, D. N. Kennedy, R. C. McKinstry, B. R. Buchbinder, R. M. Weisskoff, M. S. Cohen, J. M. Vevea, T. J. Brady, and B. R. Rosen, Science **254**, 716–719 (1991).
[2]S. Ogawa, R. S. Menon, D. W. Tank, S.-G. Kim, and H. Merkle, Biophys. J. **64**, 803–811 (1993).
[3]D. J. Brooks, J. Neurol. Sci. **115**(1), 1–17 (1993).
[4]B. E. Hammer, U. S. Patent Number 4,939,464: July 3, 1990.
[5]S. E. Derenzo, W. W. Moses, H. G. Jackson, B. T. Turko, J. L. Cahoon, A. B. Geyer, and T. Vuletich, IEEE Trans. Nucl. Sci. **36**, 1084–1089 (1989).
[6]R. Lecomte, J. Cadorette, A. Jouan, M. Heon, D. Rouleau, and G. Gauthier, IEEE Trans. Nucl. Sci. **37**, 805–811 (1990).
[7]K. Yamamoto, Y. Fujii, Y. Kotooka, and T. Katayama, Nucl. Instr. Meth. A **253**, 542–547 (1987).
[8]E. Gramsch, K. G. Lynn, M. Weber, B. DeChillo, and J. R. McWilliams, Nucl. Instr. Meth. A **311**, 529–538 (1992).
[9]M. E. Phelps, E. J. Hoffman, S.-C. Huang, and M. M. Ter-Pogossian, J. Nucl. Med. **16**, 649–652 (1975).
[10]Z. H. Cho, J. K. Chan, L. Ericksson, M. Singh, S. Graham, N. S. MacDonald, and Y. Yano, J. Nucl. Med. **16**, 1174–1176 (1975).
[11]T. F. Budinger, S. E. Derenzo, R. H. Huseman, W. J. Jagust, and P. E. Valk, Acta Radiol. **376**, 15–23 (1991).
[12]G. J. Muehllehner, Nucl. Med. **17**, 757 (1976).
[13]G. L. Brownell, C. A. Burnham, C. W. Stearns, D. A. Chesler, A.-L. Brownell, and M. R. Palmer, Int. J. Imag. Sys. Technol. **1**, 207–217 (1989).
[14]S. DeBenedetti, C. E. Cowan, W. R. Konneker, and H. Primakoff, Phys. Rev. **77**, 205–212 (1950).
[15]Radiological Health Handbook, U. S. Department of Health, Education, and Welfare, Rockville, MD, 1970.
[16]S. E. Derenzo, Proc. 5th Int. Conf. Positron Annihil., Lake Yamanaka, Japan, pp. 819–823 (1979).
[17]H. Iida, I. Kanno, S. Miura, M.Murakami, K. Takahashi, and K. Uemura, IEEE Trans. Nucl. Sci. **33**, 597–600 (1986).
[18]M. Schwartz, *Principles of Electrodynamics* (McGraw Hill, New York, 1972), p. 170.
[19]D. Evans, *The Atomic Nucleus* (McGraw Hill, New York, 1955), pp. 627–628.